HAL
open science

Magnetic phase diagram of the S=1/2 triangular layered compound NaNiO2: a single crystal study

Sophie de Brion, Markus Bonda, Céline Darie, Pierre Bordet, Ilya Sheikin

To cite this version:

Sophie de Brion, Markus Bonda, Céline Darie, Pierre Bordet, Ilya Sheikin. Magnetic phase diagram of the S=1/2 triangular layered compound NaNiO2: a single crystal study. Journal of Physics: Condensed Matter, 2010, 22 (12), pp.126001. 10.1088/0953-8984/22/12/126001 . hal-00459169

HAL Id: hal-00459169

https://hal.science/hal-00459169v1

Submitted on 10 Mar 2010

HAL is a multi-disciplinary open access archive for the deposit and dissemination of scientific research documents, whether they are published or not. The documents may come from teaching and research institutions in France or abroad, or from public or private research centers.

L'archive ouverte pluridisciplinaire **HAL**, est destinée au dépôt et à la diffusion de documents scientifiques de niveau recherche, publiés ou non, émanant des établissements d'enseignement et de recherche français ou étrangers, des laboratoires publics ou privés.

Magnetic phase diagram of the S=1/2 triangular layered compound $NaNiO_2$: a single crystal study

S de Brion[1], M Bonda[2], C Darie[1], P Bordet[1] and I Sheikin[2]

1 Institut Néel, CNRS and Université Joseph Fourier, BP166, F-38042 Grenoble cedex 9, France

E-mail: `sophie.debrion@grenoble.cnrs.fr`

2 Grenoble High Magnetic Field Laboratory, CNRS, BP166, F-38042 Grenoble cedex 9, France

Abstract. Using magnetic torque measurement on a $NaNiO_2$ single crystal, we have established the magnetic phase diagram of this triangular compound. It presents 5 different phases depending on the temperature (4 K - 300 K) and magnetic field (0 - 22 T) revealing several spin reorientations coupled to different magnetic anisotropies.

PACS numbers: 71.27+a, 75.30.Gw, 73.30Kz

1. Introduction

In magnetic systems with a two dimensional triangular lattice, magnetic frustration may occur depending on the nature of the magnetic interactions and the orbitals involved. The case of $LiNiO_2$, where Ni^{3+} has half filled e_g orbitals, has been studied for a long time both experimentally and theoretically [1]. Recent progress on the understanding of the orbital and magnetic properties of this compound has been achieved thanks to an appropriate control of the non stoichiometry or doping effects since no pure samples are available. Indeed magnetic Ni^{2+} ions are substituted between the triangular planes on the Li sites creating new magnetic exchange paths. It has been shown that $Li_{1-x}Ni_{1+x}O_2$ with x=0.01 does not show long range magnetic order. Rather, a fluctuating state develops which is slowed down when Mg doping is introduced and no interplane Ni^{2+} are presents [2]. When Li is deintercalated, in Li_zNiO_2, short range incommensurate antiferromagnetic order is observed for z=3/4 and 2/3 [3]. As for the orbital part, several experimental works are in favor of the $|3z^2 - r^2\rangle$ orbital occupancy for the e_g electrons with finite range order [4] or dynamical effects [2]. Such an occupancy is indeed observed unambiguously in the parent compound $NaNiO_2$, which seems to behave more classically. It orders ferro orbitally below $\sim$ 480 K [5] and antiferro magnetically below 20 K [6]. We present here the first single crystal study of its magnetic phase diagram up to 20 T using torque measurements. We show that several spin reorientations occur as a function of temperature or magnetic field with unusual magnetic anisotropy.

2. State of the art on $NaNiO_2$

$NaNiO_2$ crystallises in the R-3m space group and, below the ferro orbital ordering temperature, becomes monoclinic (C2/m) with a=5.3087 Å, b=2.8413 Å, c=5.5670 Å, and $\beta =$ 110.45° [7]. The two dimensional triangular network of Ni^{3+} becomes then distorted to accommodate the collective elongation of the oxygen octahedra surrounding the Ni ions (figure 1). At room temperature, the distorted triangles are described by two angles at 56.3° and 61.8° and two Ni - Ni distances at 2.84 Åand 3.01 Å. From one triangular plane to the other, the Ni-Ni distance is 5.47 Å. The antiferromagnetic ground state observed below T_{N} is of the A type with a ferromagnetic alinement of the Ni spins in the triangular plane and an antiferromagnetic alinement from one plane to the other. The magnetic moments point at 80° from the triangular planes. The Curie Weiss behavior of the magnetic susceptibility above 100K leads to ferromagnetic dominant interactions with a Curie Weiss temperature θ=+36 K. Below the ordering temperature (T_{N}=20 K), application of a magnetic field reveals a spin flop transition at $\mu_0 H_{c1}$=1.8 T [6] forT=4 K and another transition at $\mu_0 H_E$=8 T [9, 10]. Spin wave measurements agree with an easy plane A type antiferromagnet model although there are some discrepancies between the inelastic neutron measurements [8] and the electron spin resonance measurements [10]. In this model, H_E describes the strength of the antiferromagnetic coupling between the Ni planes. A small anisotropy in the easy plane

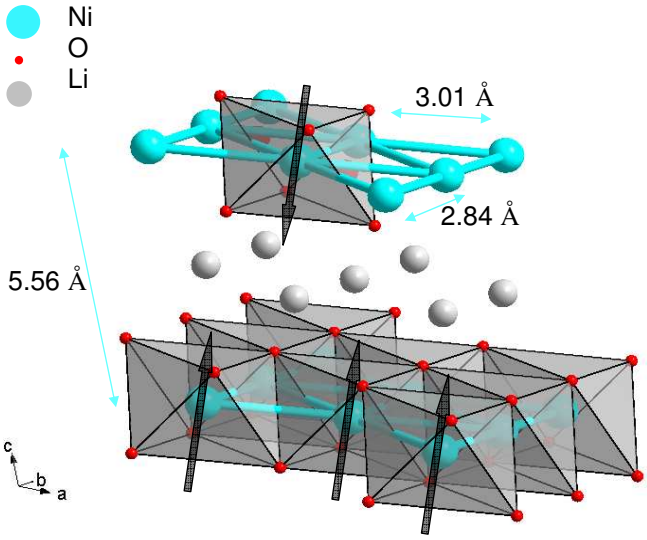

Figure 1. The triangular layered structure of $NaNiO_2$. The arrows indicate the spin directions in the zero field magnetic phase.

is then responsible for the spin flop transition at H_{c1}.

3. Synthesis of $NaNiO_2$ single crystals

$NaNiO_2$ single crystals have been grown by molten hydroxide flux method. The flux composition was NaOH and KOH, a Ni crucible played the role of Ni source. In a preliminary step, 61.6 g of a NaOH-KOH mixture (molar ratio 1:2) was melted in a separate Ni crucible at 400°C. The molten mixture was then poured in another 40 mL Ni crucible and placed in a preheated open vertical furnace. The experiment was carried out at 650°C. The evaporation of the NaOH-KOH mixture at the liquid surface induces a local saturation, then nucleation and crystal growth. Runs were stopped once an abundant "crust" was observed covering the flux surface (typically after 12 hours). The crystals were easily separated from the flux with water in an ultrasonic bath. They often take the shape of hexagonal small platelets (figure 2). The crystals were characterized using scanning electron microscopy equipped with EDX analysis (relative content: Na: 0.49 , Ni: 0.51). A mixture of crystals were crushed and studied by powder X-Ray diffraction: only stoichiometric $NaNiO_2$ was identified. Most of the crystals are twinned in the a, b plane so that the crystal platelets contain three kinds of domains with an average $c^{'}$ direction perpendicular to the platelets plane which coincides with the Ni planes.

4. Magnetic torque measurements

A sample with a magnetic moment $\overrightarrow{m}$ placed in a magnetic field $\overrightarrow{H}$ will experience a torque $\overrightarrow{\Gamma} = \overrightarrow{m} \times \overrightarrow{H}$ that can be measured using a cantilever (see figure 2). One of the larger crystals was selected (typically 1 mm x 1 mm x 0.2 mm) and glued on

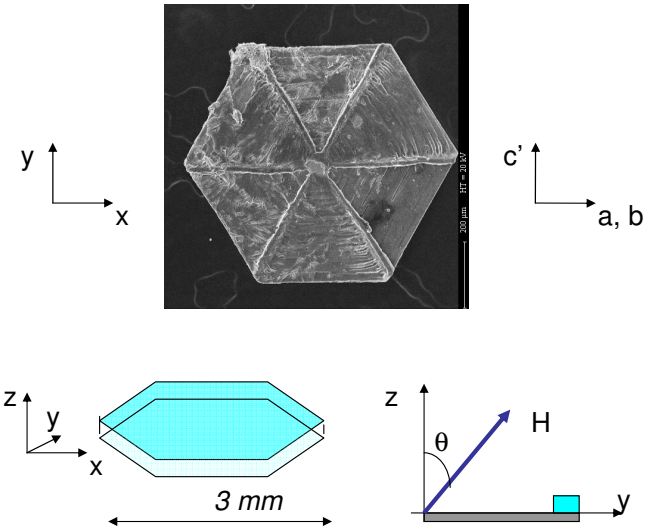

Figure 2. characteristic hexagonal shape of a 0.5 *mm* $NaNiO_2$ crystal and experimental configuration.

a copper-beryllium cantilever with General Electric varnish. Care was taken to avoid contact with air and moisture. The large face of the crystal containing the Ni planes was parallel to the cantilever (x, y) plane so that the z axis coincides with the crystal $c^{'}$ axis (see figure 2). The magnetic field H lies in the yz plane, making an angle θ with the z axis. The cantilever could rotate as regards the magnetic field so that θ could be varied from 0° to 90°. The capacitive technique allows the measurement of the torque produced in the x direction: $\Gamma_x = m_y H_z - m_z H_y$ where m is the sample magnetic moment. It is reduced to $\Gamma_x = \Delta\chi H^2 \sin(\theta - \theta_0)\cos(\theta - \theta_0)$ when the sample magnetic moment has a linear dependence on magnetic field. $\Delta\chi$ is the difference of the magnetic susceptibility parallel and perpendicular to the z axis; θ_0 is the spin direction in absence of torque. When the magnetization is saturated, the torque should vanish except for g factor anisotropy effects, which should be negligible compared to $\Delta\chi$ effects in the ordered magnetic phase.

The expected torque for $\theta = 0°$ using the easy plane model with the small anisotropy described above is given in figure 3(a), assuming that the z direction coincides with the spin direction. In the experiment, there is a 10° difference. Because of the crystal twinning, the x and y direction are not crystallographically well defined. This means that the measurement gives the average of Γ_x and Γ_y. In these calculations, the torque has a quadratic dependence on the magnetic field with a change of sign and magnitude at the spin flop field ($\mu_0 H_{c1}$=1.8 T) and vanishes at either H_{c1} or H_E. We expect then to observe three different regimes labelled (a), (b) and (c) in figure 3(a). The measured data are reproduced in figure 3(b). Four different regimes are observed and no saturation. Regime (1) has the expected quadratic field dependence and can be identified as regime (a). It disappears at H_{c1} to enter regime (2) with a change of slope, both in sign and magnitude as expected for regime (b). This transition is widen, probably due to thermal effects. Regime (b) is in fact divided in two parts, (2) and

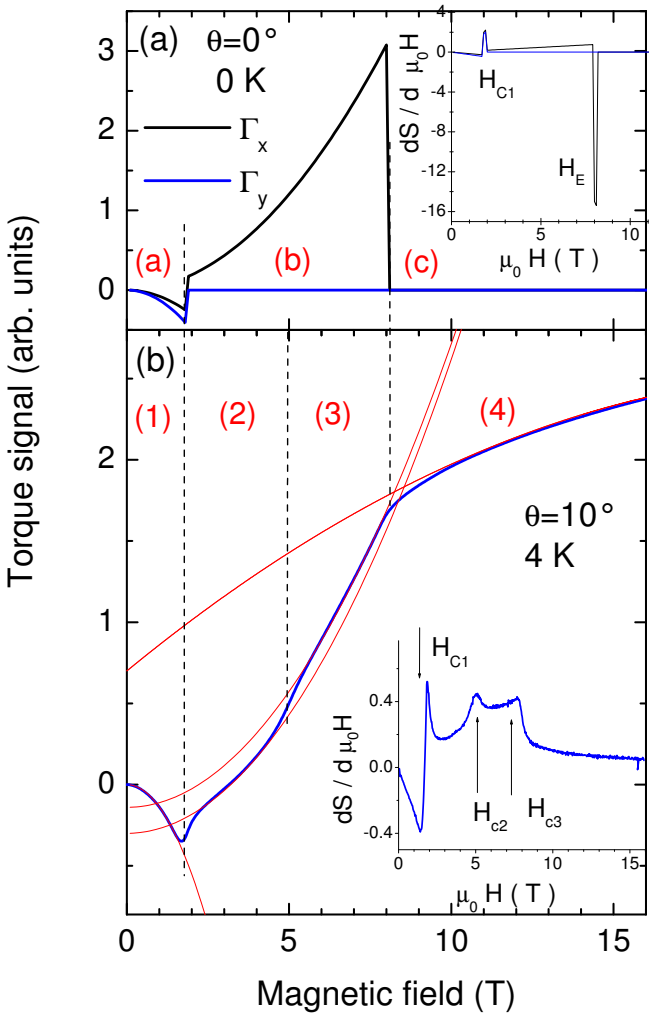

Figure 3. Magnetic field dependence of the torque on a $NaNiO_2$ crystal:(a) calculation within the easy plane model, (b) measurements and second order polynomial fits. Inserts : derivative of the torque.

(3), with similar magnetic field dependencies. Note that the quadratic field dependence for these regimes does not extrapolate to zero as calculated in regime (b) but rather there is an internal torque which has different values for regime (2) and (3). This unexpected zero field torque can exists if the extrapolated zero field magnetization is not zero (in a canted antiferromagnet for instance) or there exist local fields that are not collinear with the sample magnetization (dipolar fields due to twinning or other anisotropic fields due to crystal field effects for instance). The presence of two regimes instead of one suggests that there is a change in the anisotropy fields, i.e. a spin reorientation. The higher field regime observed, regime (4), does not saturate at all contrary to what has been calculated for regime (c). Rather, it has the following field dependence: $\Gamma_x = \Gamma_0 + \alpha(H - H_{c4})^2$ with $\mu_0 H_{c4} = 20$ T. The torque starts to decrease only above H_{c4}, which introduces another critical field in the magnetic phase diagram of $NaNiO_2$. There is an internal torque in this regime as in regime (2) and (3) with

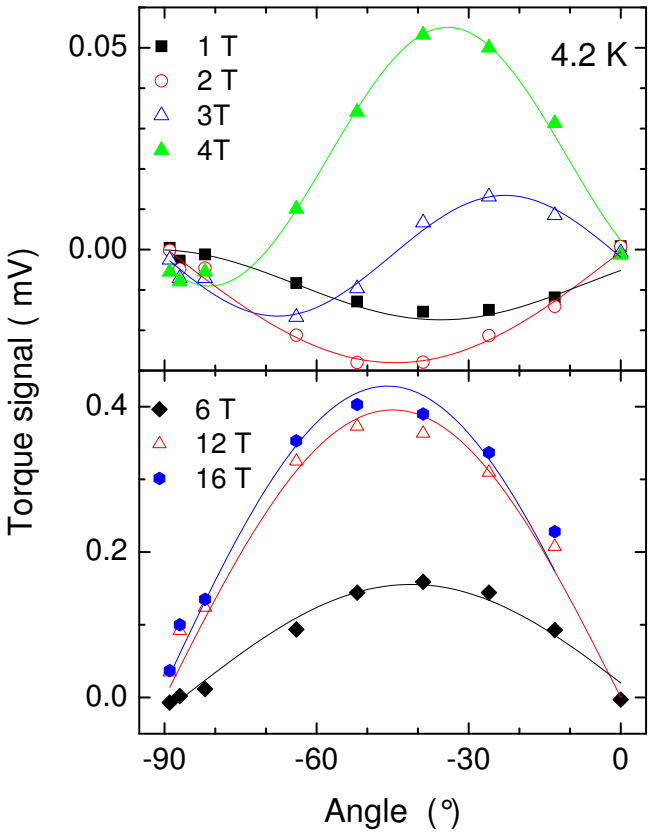

Figure 4. Angular dependence of the torque on the $NaNiO_2$ crystal at different field values

a different value. Note that these internal torques do not exist at zero field since the corresponding magnetic phases exist only at higher field. A domain pattern would have developed to compensate it and have the crystal at rest.

We have investigated more deeply each regime looking at their dependence on the magnetic field orientation (see figure 4). The low field regime, regime (1), does not follow at all the expected $\sin(\theta-\theta_0)\cos(\theta-\theta_0)$ law. Rather, it behaves as $(1-\sin 3.2(\theta-105°))$ with a periodicity of 110°. The origin of such a weird periodicity remains unclear. The presence of an incommensurate magnetic phase is to ruled out since neutron diffraction data at zero field are unambiguously fitted within a commensurate magnetic structure. On the other hand, 110° is exactly the monoclinic (a, c) angle of the crystal structure. Macroscopic effects linked to twinning are then probably responsible but difficult to evaluate due to the low symmetry of the system. Note that the critical field at which this regime disappears has the following angular dependence: $H_{c1}(\theta) = H_{c1}/\cos(\theta-\theta_{01})$ with $\mu_0 H_{c1}$=1.7 T in agreement with previous measurements [1, 6]. The free spin direction is at $\theta_{01} = -10°$ in agreement with the neutron diffraction data [7].

Regime (3) has the correct angular dependence: $\Gamma_(\theta) = \Gamma_0 \sin(\theta-\theta_0)\cos(\theta-\theta_0)$ with θ_0 close to 0°. Regime (2) seems intermediate between regime (1) and (3) with a constant evolution of the angular periodicity.

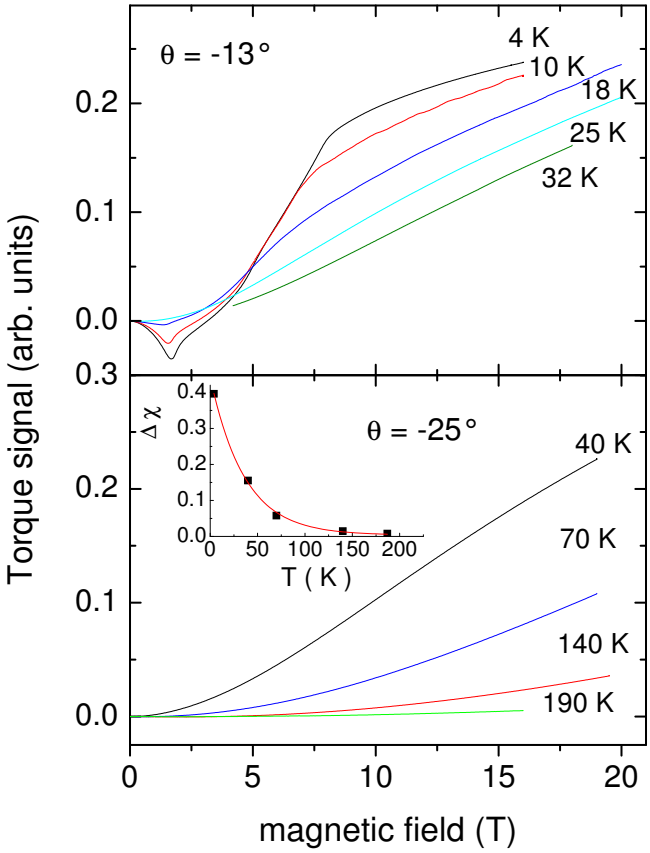

Figure 5. Magnetic field dependence of the torque at different temperatures. Insert: torque parameter $\Delta\chi$ as a function of temperature, the red line is an exponential fit.

The critical fields H_{c2} and H_{c3} at which regime (2) and (3) disappear follow the same angular dependence: $H_c(\theta) = H_c/\cos((\theta-\theta_0)/2)$ with $\mu_0 H_{c.2}$=5.1 T, $\mu_0 H_{c3}$=7.4 T, $\theta_{02} = -10°$ and $\theta_{03} = +30°$. This confirms the spin reorientation process from regime (2) to (3). H_{c3} is in agreement with the powder data ([9, 10, 11]) while H_{c2} was not detected previously.
Finally, regime (4) follow the $\sin(\theta - \theta_0)\cos(\theta - \theta_0)$ law with θ_0 close to 0°. We have checked that the field dependence remains the same for all angles, with a constant value for $\mu_0 H_{c4}$ around 20 T.

5. Discussion

These torque measurements on a twinned crystal reveal that the $NaNiO_2$ system presents several spin reorientations, and very unusual magnetic anisotropies depending on magnetic field. The modelization is quite complex due to the low crystal symmetry of the compound (monoclinic unit cell) and the presence of 3 types of twins. Nevertheless, we can establish a magnetic phase diagram using these torque measurements at different temperatures (see figure 5) . As the ordering temperature is approached, regime (1) disappears together while regime (2) and (3) merge into another regime. Note that

the torque diminishes as the temperature increases but has still a non vanishing field dependence. We checked that it behaves as $\Gamma_x = \Delta\chi H^2 \sin(\theta - \theta_0)\cos(\theta - \theta_0)$ and noticed that $\Delta\chi$ decreases exponentially with an activation energy exactly equals to the Curie Weiss temperature +36 K (see insert of figure 5). One concludes that there is a magnetic anisotropy induced by the exchange energy. It is responsible for the high field torque observed at low temperature which tends to vanish only above H_{c4}.

We can now establish the magnetic phase diagram. We have plotted in figure 6 the critical fields obtained in this work as well as in previous studies mainly on powder samples [9, 11] except for the first magnetization measurements which were taken on a twinned crystal up to 3 T [6]. At low temperature, 5 phases are present: phase (1) where the spin lies at 10° from the Ni plane, phases (2) and (3) with different spin orientations, and finally phases (4) and (5) which are close to full saturation. Phases (1),(2) and (3) disappear at $T_{\rm N} = 20\ K$ but a cross over line persists above. This phase diagram was obtained when the magnetic field was at 10° from the z axis. All the boundary lines correspond, to a good approximation, to the phase diagram when the magnetic field lies in the free spin direction i.e. -10° for phase (1), +30° for phase (3), except for the transition between phase (4) and (0) where the border line shifts to lower temperatures when θ is changed, in agreement with the specific heat data on a powdered sample [9] where a quasi vertical line is observed. While most of the phase diagram was already established, we have shown, using torque measurements on a crystal, that two additional phases are present at low temperature, phases (3) and (5). The transition line to phase (5), $H_{c4}(T)$, is obtained from the fit of the torque field variations. Since it is not a direct experimental measurement, its uncertainty is wider than for H_{c1}, H_{c2} and H_{c3}. Note that $H_{c4} \simeq 20\ T$ corresponds to an energy for the S=1/2 Ni^{3+} spin of the order of 20 K, the same order of magnitude as the observed anisotropy activation energy and Curie-Weiss temperature of 36 K. As for the transition lines $H_{c2}(T)$ and $H_{c3}(T)$, which are quite close, it is tempting to identify them with the two zero field modes at 6.5 cm^{-1} and 9.0 cm^{-1} observed in the electron spin resonance measurements on a powdered sample at 4 K[10]. The associated magnetic fields can be matched to H_{c2} and H_{c3} assuming a gyromagnetic factor $g \simeq$=2.6, in reasonable agreement with the observed g value at 200 K : $g_{\parallel}$=2.03 and $g_{\perp}$=2.28. This suggests that both H_{c2} and H_{c3} are associated with the same crystallographic plane as $g_{\perp}$ (perpendicular to the elongation axis of the oxygen octahedra). Note also that the presence of these two modes at 6.5 cm^{-1} and 9.0 cm^{-1} cannot be explained in an easy plane A type antiferromagnetic model with only two magnetization sublattices [10]. The inadequacy of this model is confirmed by our torque measurements in regime (2) and (3) where an internal torque has to be added to the model.

6. Conclusion

The magnetic study of a millimeter size $NaNiO_2$ crystal was achieved successfully using torque measurements. We have established the presence of 5 different ordered phases

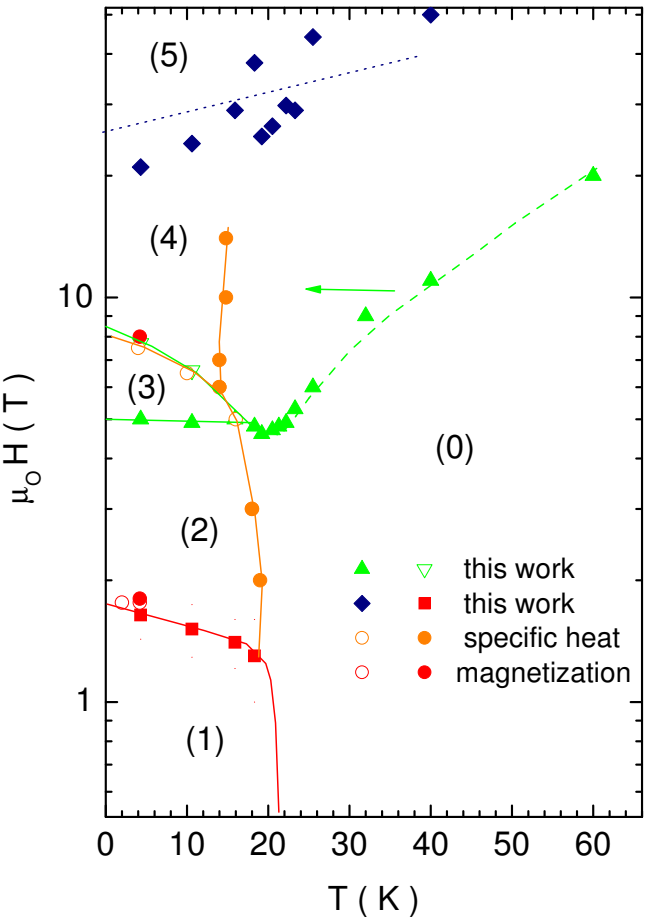

Figure 6. Magnetic phase diagram of $NaNiO_2$ from crystal torque measurements obtained at $\theta = 10°$, heat capacity ([9])and magnetization ([6, 11]) measurements.

with different spin orientations and magnetic anisotropies. The corresponding critical magnetic fields are 1.8 T, 5.1 T, 7.4 T and ∼20 T at 4 K. These reflect the presence of several characteristic energies in the system at around 2.5 K,7.5 K, 11 K and 30 K. A more complex behavior is observed than a simple easy plane A type antiferromagnet with probably different possible magnetic ground states quite close in energy.

[1] de Brion S, Núñez-Regueiro M D and Chouteau G 2005 *Frontiers in magnetic materials* (Springer Verlag) p 247
[2] Bonda M, Holzapfel, de Brion S, Darie C, Fehér T, Baker P J, Lancaster T, Darie C, T. Fehér, Baker P J, Lancaster T, Blundell S J and Pratt F L 2008 *Phys.Rev*.B **78**104409
[3] Sugiyama J, Muai K, Ikedo Y, Nozaki H, Russo P L, Andreica A, Amato A, Ariyishi K and Ohzuku T 2008 *Phys.Rev*.B **78**144412
[4] Chung J H, Proffen Th, Shamoto S, Ghorayeb A M, Croguennec L, Tian W, Sales B C, Jin R, Mandrus D and Egami T 2005 *Phys.Rev*.B **71**064410
[5] Chappel E, Núñez-Regueiro M D, Chouteau G, Isnard O and Darie C 2000 *Eur. Phys. J. B*, **17** 615
[6] Bongers PF and Enz U 1966 *SolidStateCommun*. **4** 153
[7] Darie C, Bordet P, de Brion S, Holzapfel M, Isnard O, Lecchi A, Lorenzo J E and Suard E 2005

Eur. Phys. J. B,**43** 159

[8] Lewis M J, Gaulin B D, Filion L, Kallin C,BerlinskyA J, Dabkowska H, Qiu T and Copley J R D 2005 *Phys.Rev*.B **72** 014408

[9] Baker P J, Lancaster T, Blundell S J, Brooks M L,Hayes W, Prabhakaran D and Pratt F L 2005 *Phys.Rev*.B **72** 104414

[10] de Brion S, Darie C, Holzapfel M, Talbayev D, Mihály L, Simon F, Jánossy A and Chouteau G 2007 *Phys.Rev*.B **75** 094402

[11] Holzapfel M, de Brion S, Darie C, Bordet P, Chappel E, Chouteau G, Strobel P, Sulpice A and Núñez-Regueiro M D 2004 *Phys.Rev*.B **70**132410